AIAA JOURNAL
Vol. 45, No. 4, April 2007

Development of a Kinetic Nucleation Model for a Free-Expanding Argon Condensation Flow

Jiaqiang Zhong* and Deborah A. Levin*
Pennsylvania State University, University Park, Pennsylvania 16802

DOI: 10.2514/1.28234

Using classical nucleation theory (CNT), a homogeneous condensation model has been developed in previous work to simulate condensation in a free-expanding plume using the direct simulation Monte Carlo (DSMC) method. However, the accuracy of the CNT nucleation theory is questionable due to unphysical assumptions such as the use of macroscopic cluster surface tension for small clusters and the lack of an incubation time for nucleation. Molecular dynamics (MD) simulations performed in previous work confirm that the fundamental mechanism for the initiation of condensation is through dimer formation in two-stage ternary collisions of monomers. In this work we propose a kinetic nucleation model based on the mechanism whereby stable dimers are created from triple collisions. The new hybrid MD-DSMC kinetic nucleation model is implemented in a DSMC simulation of cluster growth processes, starting from dimers, in a condensation plume. Comparison of the distributions of steady-state plume cluster number density and size using the kinetic and CNT nucleation models shows that the condensation physics is significantly different for the two nucleation models investigated. The use of a physically more realistic nucleation model is shown to generate terminal cluster properties consistent with experiments in free-expanding jets.

Nomenclature

A	=	atom species, or constant
C_1	=	constant
C_2	=	constant
d	=	nozzle throat diameter
E	=	energy
f	=	distribution function
k	=	Boltzmann constant
N_c	=	number of clusters, or number of collisions
n_v	=	gas number density
P	=	pressure, or probability
R	=	radius of the collision cross section, or collision rate
r	=	impact parameter
T	=	temperature
v	=	collision relative velocity
Γ	=	degree of condensation
ϵ	=	potential well depth
μ	=	reduced mass
ν	=	collision frequency
σ	=	potential constant, or collision cross section
τ	=	collision duration time
χ_2	=	dimer mole fraction

Subscripts

d	=	dimer
t	=	translation state, or triple collision
0	=	stagnation state

I. Introduction

CLUSTER formation processes are all-encompassing and found in countless applications important to society: medical research, creation of new and novel materials, and developing low-cost space-based worldwide telecommunications, to name a few. Detailed statistical characterization of cluster properties is important for micro- and nanoscale materials fabrication technologies such as chemical vapor deposition [1], pulsed laser deposition [2], dry etching [3], cluster deposition [4], and laser ablation [5]. Deposition of size-specific clusters opens up a new class of surface nanostructure fabrication of materials that have size-specific catalytic properties [6]. Strategies for the reduction of cluster formation in pulsed laser ablation deposition of thin films [7] demonstrate the need for control of the size of clusters in the vicinity of a target surface.

Condensation coupled flow plays a role in the highly complex problem of spacecraft contamination. Hydrazine propellant reaction control thrusters are typically used for attitude control and station-keeping purposes and their chemical byproducts typically include many of the simple gases [8]. Modeling of condensation phenomena within the plumes of these thrusters is the first step towards predicting size distributions of conglomerates of larger particles [9], which can ultimately harm sensitive surfaces of the spacecraft. Harvey [10] shows the serious effects of hydrazine thruster contamination for an actual solar cell array panel that was on used Mir for more than a decade. Because solar cell arrays are a crucial spacecraft system, the arrays must be oversized to account for the damaging effects of contamination. This work represents our continuing efforts to quantitatively model homogeneous condensation in rarefied transitional flows that are relevant to the space environment.

Application of kinetic methods to condensation has been an important subject of fundamental research in the physics of two-phase flows. For example, Ishiyama et al. [11] applied the molecular dynamics approach to study argon gas condensation behavior on a single argon cluster in equilibrium states. Meland et al. [12] also used a molecular dynamics approach to study 1-D gas flow condensed onto a liquid surface. Recently, Frezzotti et al. [13] used a direct simulation Monte Carlo (DSMC) approach to simulate condensation of a polyatomic gas on a planar surface in a 1-D flow. In that work [13], an assumed value for the condensation coefficient was used to numerically study the impact of freestream Mach, temperature, number of gaseous molecular rotational degrees of freedom, and condensation coefficient on the gaseous pressure and temperature in the Knudsen layer. These papers [11–13] model a gas-condensate system that is relatively simple and uniform. In contrast, the main goal of this work is to study the condensation in a more complex flow of a freely expanding plume, considering cluster initiation processes and then the interactions among millions of cluster and gas particles.

In contrast to the work of [11–13], a supersonic, free-expansion flow encompasses multiple length scales and degree of saturation as

Presented as Paper 4950 at the 48th AIAA Thermophysics Conference, Toronto, 6–9 June 2005; received 6 October 2006; revision received 29 December 2006; accepted for publication 19 January 2007.

*Department of Aerospace Engineering

the gas density rapidly drops from the stagnation pressure to vacuum conditions. Because for most of the computational region the continuum assumption breaks down, a kinetic approach is required. The DSMC method of Bird [14] is employed to model both the gas as well as cluster flow. In earlier work [15], we discussed the justification for using DSMC to model the nongaseous cluster species in the flow and showed that the key assumptions of DSMC, that the gas is dilute and formed by binary collision, also hold for the cluster species.

Modeling of homogeneous condensation flows includes two main processes. The first one is the nucleation process during which the initial nuclei are created from the gas phase, and the second is the cluster growth process. Microscopic models based on kinetic collision theory and general mass, momentum, and energy conservation relationships, including cluster-monomer sticking and nonsticking collision models and cluster evaporation models, have been developed to describe cluster growth processes so that energy and momentum are conserved as the cluster size increases [15]. In our previous work, we have found that the condensation flow is most sensitive to the nucleation process [16]. Therefore, a major goal of this work is to develop and apply a physically correct nucleation model to a full plume system expanding flow.

Several approaches applicable for describing the formation of initial clusters in a supersaturated gas environment have been reported in the literature. The first approach, based on the classical nucleation theory (CNT) [17], assumes that the initial clusters, referred to as the critical clusters, are born in an equilibrium state with the ambient gas during the density fluctuation process. Though the critical cluster is larger than the minimum cluster, a dimer, CNT theory neglects the question as to how the dimers are born from monomers and how the dimers grow to the size of the critical clusters. Although easy to implement, the accuracy of CNT theory is questionable [18] because it assumes a constant gas number density, a maximum cluster size, and a steady-state and isobaric/isothermal gas environment during the nucleation process. The CNT nucleation rate is also very sensitive to macroscopic parameters [19], especially cluster surface tension, which may not even be applicable or poorly known for small clusters. Because of these intrinsic disadvantages, several orders of magnitude error in the CNT nucleation rate has been reported in the numerical molecular dynamics (MD) simulations [20,21] and experimental work [22].

Another approach, referred to as the kinetic approach, treats nucleation as a process of kinetic chemical aggregation [18]. Yasuoka and Mastumoto [20] used an MD approach to obtain an argon nucleation rate, assuming that the cluster is defined to exist when the intermolecular distance is less than a reference value. Senger et al. [21] used a Monte Carlo (MC) method to calculate the nucleation rate in argon, and the cluster in his work is characterized as intermolecular connectivity distance and a mean volume within which the cluster molecules must reside to separate from the surrounding gas molecules. Based on variational transition state theory (TST), Schenter et al. [23] developed the vapor phase nucleation rate in terms of Helmholtz free energy. In the TST nucleation theory, an optimized dividing surface is defined for each cluster, separating product states from reactant states, and the nucleation rate can be obtained from the equilibrium reactive flux across the dividing surface.

Because dimers are the precursors for trimers, quadrimers, and other larger clusters, the fundamental challenge to modeling nucleation is essentially resolving how a dimer is formed in the gaseous environment. A physically plausible scenario of nucleation involves three-body or triple collisions in which the seed clusters, stable dimers can be formed from two of the three colliding monomers while the other monomer takes away the excess energy [24]. In molecular dynamics simulations of a free-expanding core plume [25,26], dimers were observed to form through triple collisions, consistent with the interpretation of experiments by Knuth [27]. In this work we use this finding to develop a nucleation model that creates initial clusters, dimers, from triple collisions and then studies their growth in a free-expanding argon plume. Note that after the initial clusters are created from the gas molecules, the interactions among clusters and gas molecules, for example, sticking and nonsticking collisions, are modeled in the DSMC expanding flow and are based on MD simulations discussed in earlier work [28,29].

As mentioned, the DSMC [14] approach has been chosen to simulate homogeneous condensation in free-expanding plumes due to the rarefied nature of the flow [15,28]. Though the DSMC method is theoretically based on the binary collision assumption, the implementation of the triple collision has been proposed by Bird [14] and Boyd [30] to model chemical reaction processes. To model a triple collision in the DSMC approach, a lifetime has to be assigned to a binary pair, known as a collision complex. Three-body collisions are then treated as subsequent collisions between the complex and monomers during the complex lifetime. The accurate estimation of the complex lifetime is a challenging task because it relates to the intermolecular force, molecular relative velocity, and collision impact parameter. Furthermore, the reaction probability of a triple collision is usually unknown although the binary reaction probabilities can be approximated from the empirical Arrenhius rate equation [31]. Finally, to calculate atomic O recombination probability P_t as a two-step binary collision process in an argon environment, Koura [32] introduced an artificial test particle with a collision cross section approximately equal to the sum of molecular vibration and rotation cross sections. Koura defined the recombination probability as the ratio of the real collision frequency to a virtual value. This present paper, to the best of our knowledge, is the first work to use kinetic MD and 0-D DSMC approaches to obtain the complex lifetime and triple collision reaction probabilities, and the first work to apply the kinetic results and the complex lifetime and triple collision reaction probabilities in the DSMC simulation to model the cluster nucleation process through the triple-collision processes.

The present paper is organized as follows: An MD technique is applied in Sec. II to directly simulate 1-D free-expansion flow, and it confirms that the fundamental mechanism for the initiation of condensation is through dimer formation in two-stage ternary collisions of monomers. In Sec. III, a hybrid MD-DSMC approach is used to obtain the probability of generating an initial dimer from a triple collision. First, MD is employed to simulate the complex lifetime as a function of collision impact parameter and relative velocity. Then a 0-D DSMC calculation is used to simulate the number of collisions between collision complex and argon molecules. The kinetic nucleation model obtained in Sec. III is then applied in Sec. IV to a free-expanding plume. In this method, homogeneous condensation is initiated from the dimers formed out of the triple collisions. The steady-state solutions for the distributions of cluster size and number density are compared with those obtained from simulations using the CNT nucleation process and the experimentally derived relationship of Knuth [27] for terminal dimer mole fraction.

II. Physical Evidence of the Proposed Dimer Nucleation Process

A realistic scenario of the nucleation process is the dimer formation from monomers, which should involve an energy loss mechanism such as the interaction with a third monomer in a three-body collision [24]. Knuth [27] has shown that a consecutive collision of a monomer with an orbiting complex of two other colliding monomers (the two-stage ternary collision) is plausible for dimer formation in supersonic jets; however, there is no direct evidence that the formation of initial clusters in nonequilibrium gas starts from dimer formation in ternary monomer collisions.

A direct, straightforward simulation of condensation in free gas expansions will facilitate the understanding of a microscopic mechanism of condensation in nonequilibrium flows. Unfortunately, the application of a direct method, such as MD, to the simulation of the entire expansion region of even small gas-expansion systems, for example, a supersonic jet, is not possible. This is because the number of MD particles would be at least of the order of 10^{12} and these particles must be followed for several microseconds [25], whereas the typical values accessible in MD are 10^6 particles and a few

nanoseconds of simulated time [33]. We will implement the MD technique to simulate not the entire supersonic jet system, rather, a 1-D gas expansion [26], which will greatly reduce the computational cost.

The initial system geometry of our MD simulation region, a closed reservoir, corresponds to a small thin bar, $280 \times 25 \times 25$ nm, with periodic boundary conditions (PBC) on all six surfaces to reduce the dependence on the number of particles used in the simulation. To accurately simulate the open reservoir conditions, the periodic boundary on the right-hand transversal (25×25 nm) surface is replaced by a free boundary, and the left-hand transversal surface boundary condition becomes reflective. In a qualitative sense, the location of the free boundary corresponds to an orifice in a full reservoir-nozzle system. It can be shown that only a small fraction of particles exit the reservoir such that the pressure in most parts of the reservoir is constant during the total computational time (approximately 400 ps) [26].

The main challenge in direct MD simulations is to find sufficient numbers of clusters in the plume during the accessible simulation time [25]. We, therefore, choose the argon stagnation conditions of 2 atm and 65 K corresponding to a supersaturated state in the following simulations of a free gas expansion. A series of simulation "snapshots" is depicted in Fig. 1. During the simulation time, gas expands over about 1000 Å in the axial direction and becomes rarefied. The number of particles clearly decreases with the distance from the orifice whose X coordinate is 1400 Å. At the same time, the axial distance between particles gets larger due to the expansion process as the distance from the orifice increases. The macroscopic parameters, such as the number density, temperature, and Mach number, obtained from the MD simulations, quantitatively agree with the analytical solutions within the entire computational domain [26]. Thus, the MD simulation results correctly capture the physics of the expanding flow.

In MD simulations, each particle has a unique identification number (ID) that is kept constant throughout the simulation. To separate actual clusters from randomly colliding atoms, we first identified clusters in the plume region for each "snapshot" file using the Stillinger criterion [34]. The time separation of 10 ps between the snapshots is larger than a typical collision time [25], so that by comparing the IDs of cluster atoms in two successive snapshots, we can eliminate the colliding pairs. Then we track the history of each cluster to separate clusters originated in the plume from those formed in the reservoir. For example, two atoms appear as a dimer both at 360 and at 370 ps, then the status of these atoms should be checked also at 350 ps, 340 ps, etc., until both atoms are identified as monomers. In analyzing the origins of clusters, it was found that clusters originate from two-stage ternary collisions (TSTC) [26]. Based on these numerical results, it may be concluded that the condensation in free gas expansions starts from the formation of dimers in the two-stage ternary collisions of monomers, as was assumed previously by many researchers.

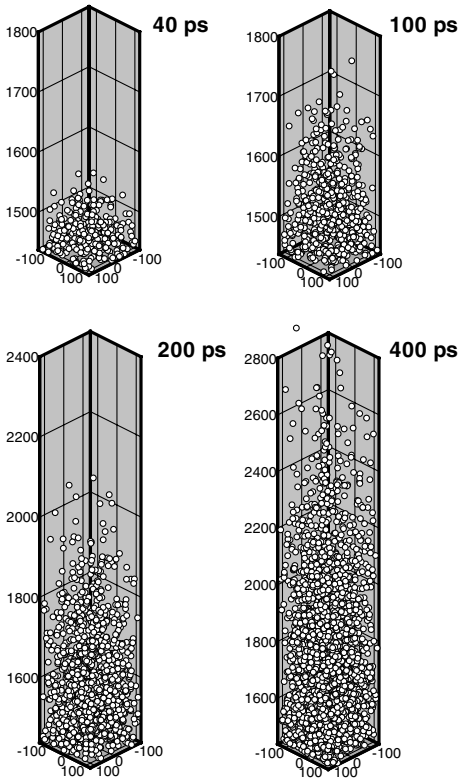

Fig. 1 A series of simulation snapshots. The orifice vertical coordinate is 1400 Å.

III. Modeling of Dimer Formation, a Hybrid MD-DSMC Approach

To simulate condensation flow with a kinetic nucleation approach, the initial clusters, dimers, have to be created from triple collision processes. Three molecules may collide together as follows [35]:

$$A + A + A \xrightarrow{k_f} A_2 + A \tag{1}$$

where A_2 represents a stable dimer created from a triple collision and k_f is the forward rate constant for the triple collision process.

The probability of process (1) could be derived from triple reaction rate, a pure MD study and a hybrid 0-D MD-DSMC method. The first two approaches and their respective limitations are briefly reviewed, then we present the 0-D MD-DSMC method used in this work. The probability P_t of creating stable dimers out of triple collisions is related to k_f as [30]

$$n_v k_f = \overline{\sigma v} \int_0^\infty P_t(E_t) f\left(\frac{E_t}{kT}\right) \mathrm{d}\left(\frac{E_t}{kT}\right) \tag{2}$$

where σ is the monomer–monomer collision cross section, v is the monomer–monomer collision relative velocity, and $f(\frac{E_t}{kT})$ is the collision energy distribution function. Kalus [36] suggests that the argon forward rate constant, k_f, may be fitted into a non-Arrhenius formula according to trajectory simulation results,

$$k_f = AT^{C_1} \exp(-C_2 T) \tag{3}$$

where T is gas temperature over a 15–500 K range, the value of constant A is approximately 1.015×10^{-43} m^6/s, C_1 is -0.278, and C_2 is -3.1×10^{-3}. Using Eqs. (2) and (3), the average probability $\bar{P}_t$ based on the equilibrium Maxwellian distribution function is about 0.06–0.08 for the gas environment to be discussed in Sec. III.B. Note that the accuracy of Eq. (3) needs to be further validated in temperature regions below 100 K due to its poor agreement with the simulation results. Furthermore, because the collisions usually occur among molecules with larger relative collision velocity, the probability averaged over entire distribution function, $\bar{P}_t$, is not accurate.

The probability P_t could potentially be computed directly from MD simulations by tracing each molecular position, momentum, and energy, and counting the number of triple collisions and stable dimers based on a geometric criteria [34,37] and history tracking method [25]. To count the number of triple collisions in an MD system, the relative distance among simulated particles need to be calculated continuously to determine whether a triple collision has occurred. This leads to a high computational cost that makes the separation of triple collisions from the dimer–monomer collisions a challenging MD simulation.

In this work, we propose a hybrid MD-DSMC approach to obtain the probability of creating stable dimers from triple collision, as will be discussed in Sec. III.B. Because the number of stable dimers and the number of triple collisions are directly counted in the 0-D MD and DSMC simulations, the probability P_t can be calculated from the hybrid MD-DSMC approach with less computational cost compared to the pure MD method, and without the assumption of a Maxwellian

distribution function necessary to use the reaction rates if Eq. (2) were used.

To implement triple collisions in a DSMC simulation, the triple collision shown in Eq. (1) has to be decomposed into two successive binary collision steps as [32,38]

$$A + A \rightarrow A_2^* \tag{4}$$

and

$$A_2^* + A \rightarrow A_2 + A \tag{5}$$

The atom–atom binary collision (A–A) generates a temporary pair A_2^* with a lifetime that is approximately equal to the binary collision duration. The pair A_2^*, known as a collision complex, may collide with a third monomer during its lifetime to create a stable dimer, as indicated in Eq. (5).

In the DSMC method, collision pairs must be selected from the simulated gas particles in a computational cell and, if chosen, the outcome of the collision is evaluated. This process could be time-consuming because the number of collision pairs is proportional to N^2, where N is the number of simulated particles. To decrease the computational cost, the no time counter (NTC) [14] and majorant frequency (MF) [39] schemes have been developed to numerically decrease the number of candidate collision pairs, while increasing the probability for an accepted collision. In this work, we use the DSMC-based SMILE [39] code, which uses the MF scheme for selecting collision pairs. The majorant collision frequency ν is given by [40]

$$\nu = [F_n N_c (N_c - 1)/2]\{\sigma(v)v\}_{\max} \tag{6}$$

where N_c is the number of molecules in a cell and $\sigma(v)$ is the total cross section based on the variable hard sphere model for gas molecule collisions. The collision probability for collision pairs selected from Eq. (6) is

$$\frac{\sigma(v)v}{\{\sigma(v)v\}_{\max}} \tag{7}$$

The procedure of modeling the triple collision in two separate steps in a DSMC scheme that will be used in this work may be summarized as follows: The number of atom–atom collision pairs is calculated using the original DSMC scheme, Eq. (6). For an accepted atom–atom collision pair, defined as a collision complex A_2^*, the number of A_2^*-atom collision pairs is further calculated during the A_2^* lifetime. Note that the center of mass velocity of the atom–atom collision pair is assumed to be the A_2^* velocity and the value of A_2^*-atom collision $\sigma(v)$ is assumed to be constant and equal to $\sigma(v) = \pi(\frac{d_* + d_0}{2})^2$, where the atom diameter $d_0 = 4.17$ Å and A_2^* diameter d_* is assumed to be $2d_0$. Note that complexity of the cluster–monomer collision model could be increased. However, molecular dynamics studies of cluster–collision cross sections reported in earlier work [28] for expanding flow conditions similar to those that will be discussed in this work demonstrated good agreement with the hard sphere model. As in the traditional DSMC method, the acceptance-rejection principle is used to evaluate whether the A_2^*-atom collision, referred to as the triple collision in this work, occurs or not. For a successful triple collision, if the selected random number is less than the probability P_t, a dimer would be created and at the same time two atoms out of the initial three colliding atoms would be consumed. To avoid introducing artificial test particles as was done in [32], we define the probability P_t in this work as the ratio of the number of stable dimers to total number of A_2^*-atom collisions. The A_2^* lifetime and the probability P_t are obtained as follows.

A. MD Simulations of the A_2^* Lifetime

To obtain the complex lifetime, the MD method is chosen to simulate various binary collision processes corresponding to the initial conditions that will ultimately be needed in the DSMC simulations. The intermolecular force between argon atoms is calculated from the 6–12 Lennard–Jones potential with a well depth

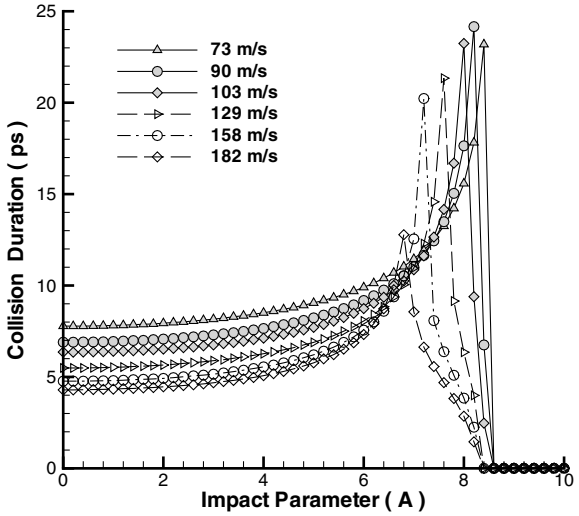

Fig. 2 MD trajectory studies of the binary collision duration as a function of the impact parameter and the collision relative velocity.

σ of 3.405 Å and ε of 0.0103 eV. A time step of 1.0×10^{-15} is used in the MD simulation. In a typical simulation case, two molecules first move freely toward each other, then collide at some range, and finally separate beyond a range where they have any interaction. The beginning and end of a collision are determined by the times at which the particle velocity first starts and then stops changing. Thus, a collision duration, assumed to be the A_2^* lifetime, may be calculated from the results of the MD trajectory simulations.

The MD simulation results of a binary collision duration for argon atoms are shown in Fig. 2 as a function of typical collision relative velocity and impact parameter. The collision duration time is regarded as the lifetime of the argon complex A_2^*. Each symbol in Fig. 2 represents one simulation case. It can be seen that for the collisions with the same relative velocity, the duration time increases as the impact parameter increases. The duration time reaches a maximum value at a critical impact parameter R, then it quickly decreases to zero for the collisions with impact parameters larger than the critical value. For the collisions with the same impact parameter, Fig. 2 shows that the duration time decreases as the relative velocity increases.

For a single relative kinetic energy, an average collision duration τ can be calculated from Fig. 2 based on an R^2 distribution of collision pairs as follows:

$$\tau = \frac{1}{R^2}\int_{r=0}^{r=R} \tau(r)\,\mathrm{d}r^2 \tag{8}$$

The value of R is seen from Fig. 2 to be a function of the collision relative velocity and was chosen as the impact parameter corresponding to the maximum collision duration time in each case.

The average collision duration obtained from the MD simulations, compared with lifetimes calculated by Bunker's approximate formula [35], are shown in Fig. 3. Bunker's formula, derived for particles that interact by the attractive part of the Lennard–Jones potential, provides the following relationship between the mean collision duration time τ, the parameters of the interaction potential ε and σ, the reduced mass μ, and the relative translational energy E_t:

$$\tau \approx \frac{3}{2}\sigma\mu^{\frac{1}{2}}\varepsilon^{\frac{1}{6}}E_t^{-\frac{2}{3}} \tag{9}$$

We can see in Fig. 3 that Bunker formula poorly describes the actual MD results indicated as the triangular symbols. Another recent MD study [38] has also shown that actual mean collision duration significantly deviates from Eq. (9). Because the MD study results show that the variation of collision time is small with respect to energy, we will use a constant value of $\tau = 10$ ps in the determination of the number of triple collisions. This value

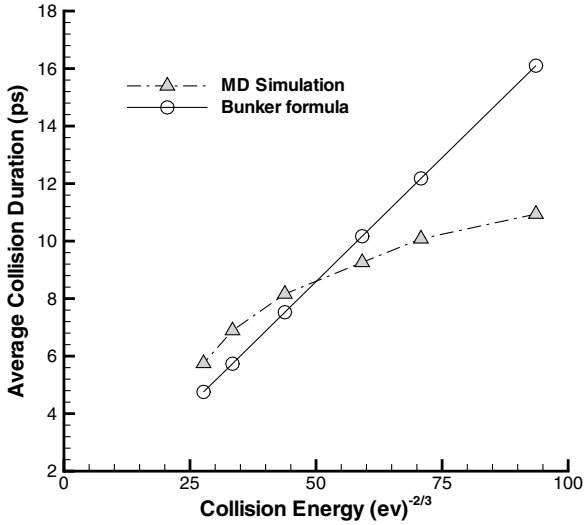

Fig. 3 Comparison between MD and the Bunker formula of average collision duration for different relative collision energies.

corresponds to a relative velocity of ~100 m/s, which is a typical condition in the expanding plume flow.

B. Probability P_t: A Combined MD and DSMC Approach

The probability P_t to form a stable dimer is defined as the ratio of the number of stable dimers, N_d, to the number of triple collisions, N_t,

$$P_t = \frac{N_d}{N_t} \tag{10}$$

In our DSMC simulations, the original collision scheme shown in Eq. (6) is used to calculate the number of A_2^*-atom triple collision "pairs" during the complex lifetime, and the probability, calculated by Eq. (7), is used to determine whether the collision pairs are accepted or rejected. A successful pair selection, followed by a successful collision, increases the number of triple collisions, N_t.

First, a series of 0-D DSMC simulations are designed to calculate the number of accepted triple collisions, N_t, for the cases shown in Table 1. We choose several spatially constant (0-D) test gas environments that are sufficiently dilute to be simulated by the DSMC approach, but not so rarefied as to generate too few stable dimers. The test gas environments, having the same number density of 1.25×10^{26} atoms/m^3, are summarized in Table 1, where T is gas temperature, P is the pressure, S is the degree of supersaturation defined as the ratio of the gas pressure to the saturation pressure, and R_t is the triple collision rate, which will be discussed later. Note that the 0-D test gas environments are conditions typical for homogeneous condensation in a free-expanding plume, with the degree of supersaturation ranging from 15 to 2200.

For all the 0-D DSMC simulations, we choose a closed computational domain of $10^{-5} \times 10^{-5}$ m with the specular boundary conditions. The computational domain is divided into square grids with a grid size of 5.0×10^{-8} m, on the order of the mean free path and a time step of 10^{-11} s is used. The number of real atoms represented by one simulated particle, F_N, is chosen to be 1.0×10^{11} in the 0-D DSMC simulations, and there are about 12,500 simulated

Table 1 Test gas environments and probabilities for dimer formation from triple collisions

No.	$T(K)$	$P(\times 10^5$ Pa)	S	$R_t(\times 10^{35}$ m$^{-3} \cdot$ s$^{-1})$	P_t
1	50	0.8625	2263.34	1.581	0.234
2	55	0.9487	459.78	1.650	0.224
3	60	1.035	119.67	1.706	0.217
4	65	1.121	40.24	1.766	0.209
5	70	1.207	15.58	1.819	0.203

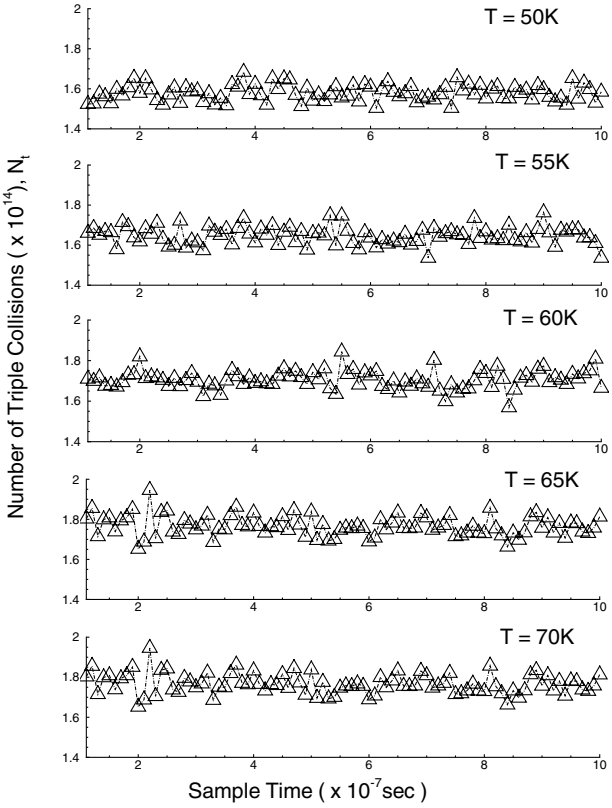

Fig. 4 The number of accepted collision pairs between a temporary complex and a monomer occurring in a $10^{-5} \times 10^{-5} \times 1.0$ m during each time step of 10^{-11} s for various temperatures.

particles for each case. As discussed earlier, each accepted atom–atom collision in the DSMC simulation is assumed to create a dimer complex, A_2^*, with a lifetime around 10 ps. The number of collisions between A_2^* and monomers (i.e., the triple collision) are counted during each time step in the 0-D DSMC simulation. Because the number of collisions counted in a DSMC simulation is for simulated particles and the number of simulated particles are inversely proportional to F_N, the total number of collisions in a real environment corresponding to $F_N = 1$ can be obtained. The number of accepted triple collisions in the computational domain during a single time step under the condition of various temperature are shown in Fig. 4, and the average triple collision rates, R_t, are shown in Fig. 5. It can be seen that as the temperature increases, the number of triple collisions also increases. Because the only purpose of these simulations is to count the number of triple collisions, the three colliding atoms in a A_2^*-atom triple collision pair are released into separated atoms whether or not the collision is finally accepted. Thus, the gas environment is always held constant and the number of triple collisions can be counted repeatedly to improve statistics.

In the second part of the combined MD-DSMC approach for obtaining P_t, molecular dynamics is used to calculate the number of stable dimers, N_d, generated from the aforementioned gas environments. Although the MD method is not able to simulate the whole DSMC domain, due to computational cost limitations, it can be used to simulate interactions among argon molecules in a spatial region on the order of one DSMC cell. A computation domain of $60 \times 60 \times 60$ nm with the same gas number density and temperatures used in the 0-D DSMC calculations is chosen. Thus there are a total of 27,000 atoms in each MD simulation and a time step of 10^{-15} s is used. Initially the simulated atoms are evenly distributed in the MD computational domain and the average distance between two atoms is about 2 nm. The initial atom velocities are sampled from the equilibrium Maxwell distribution function. The same 6–12 Lennard–Jones potential used to calculate the argon A_2^* lifetime (Sec. III.A) is used to model the interactions among argon atoms. A geometric criteria [34,37] and history tracking method [25]

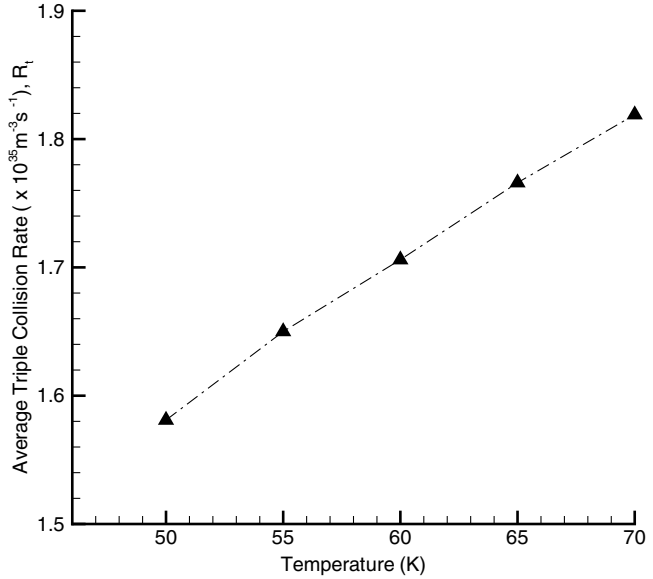

Fig. 5 Average triple collision rate per cubic meter per second under the condition of various temperatures, R_t.

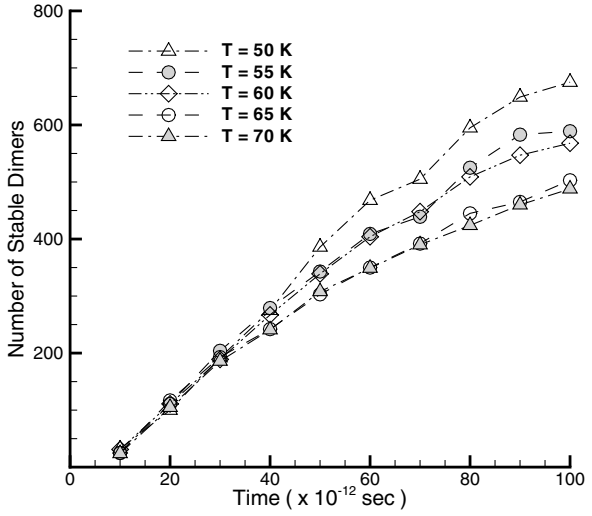

Fig. 6 The number of stable dimers, N_d, obtained in a 60 × 60 × 60 nm cubic box, under the condition of various temperature.

are used to separate stable dimers from the colliding pairs at every 10 ps. The detailed description of the numerical method is given in [25].

The number of stable dimers, N_d, found in the MD analysis as a function of simulation time are shown in Fig. 6 for different temperatures. It can be seen that as the simulation time increases, the number of dimers found in the system increases. Note that the changes in gas environments can be neglected because the number of molecules in the formed clusters is less than 5% of the total number of molecules during the MD simulations. Thus, the dimer formation rate should be almost constant and the number of stable dimers should increase linearly as a function of time. However, the nonlinear effect that can be seen in Fig. 6 beyond 50 ps is mainly due to dimer dissociation processes, especially in higher temperature gas environments. This is because a stable dimer formed in a higher temperature environment has a shorter life time, and therefore more dimers may dissociate into separate atoms in the same period of time as the temperature increases. Because our interest is to use these MD simulations to obtain the initial dimers, the dimer formation rates are calculated as the curve slopes in the first 40 ps, during which most of the dimers can survive. Note that cluster dissociation or evaporation process will be considered by one of the microscopic models in the *full* DSMC simulation. As the gas temperature increases from 50 to 70 K, the degree of supersaturation decreases approximately from 2200 to 15; however, the stable dimer formation rates are almost the same. According to Fig. 6, approximately $N_d = 80$ dimers are generated in a supersaturated gas environment every 10 ps in a cell volume of $(60\ \text{nm})^3$ corresponding to a formation rate $R_d = 3.7 \times 10^{+34}$ dimers/$(\text{m}^3 \cdot \text{s})$.

Finally the probability P_t can be calculated as the ratio of the MD dimer rate, $R_d = 3.7 \times 10^{+34}$ dimers/$(\text{m}^3 \cdot \text{s})$, to the DSMC triple collision rate, R_t, and the results are shown in Table 1. It can be seen that P_t is not very sensitive to the degree of supersaturation. To simplify the use of the P_t in the full DSMC simulations, we will choose a constant probability of 0.217.

IV. Results and Discussion

The DSMC method has been developed to simulate condensation in free-expanding plumes. In our previous work [15], the microscopic nucleation, collision, and evaporation models, as well as simulation techniques were proposed and integrated into the DSMC code to simulate cluster growth processes. To accurately model interactions among clusters and gas molecules in a DSMC simulation, molecular dynamics calculations have been used to simulate cluster–monomer and cluster–cluster collision processes [28]. In previous work the initial clusters were created from supersaturated gas environments using the classical nucleation theory. Because of the disadvantages of the CNT theory discussed in Sec. I, the kinetic nucleation procedure proposed in Sec. III will be applied in this section to model nucleation of dimers. The same collision and evaporation models presented in previous work [15,28] are used here to model the subsequent cluster growth.

Here we consider condensation in a free-expanding pure argon plume through a sonic nozzle with a stagnation pressure of 125 torr, a stagnation temperature of 280 K, and throat diameter of 3.2 mm. The details of DSMC simulation models and techniques were developed in [15], and can be briefly summarized for the simulation with a kinetic nucleation process as follows. The original 2-D axisymmetric SMILE code [39] is modified to simulate nucleation, cluster–monomer collision, and evaporation processes. The simulation domain extends 4 and 10 times the orifice diameter in the radial and axial directions, with 100 and 250 cells, respectively. Using an adaptive grid technique, each cell can be divided up to 16 subcells according to the flow gradients obtained during the simulation. The number of cells was found to increase from 25,000 to 175,000 at steady state, and a time step of 2.0×10^{-9} s is used in the DSMC simulation. To decrease the computational cost, radial weights are used for distributing the number of simulated molecules evenly in the radial direction for monomers and clusters. Because of the several orders of magnitude difference in the cluster and gas number density, one simulated cluster particle represents $5.0 \times 10^{+7}$ real clusters, and one simulated gas molecule represents $1.0 \times 10^{+10}$ real gas molecules. Our choice of species weighting factors has been tested in previous work [41] to ensure that our results are independent of their specific values. Because the noncondensation region close to the orifice is too dense to be modeled by DSMC, the simulation begins from a starting surface which is created with the continuum solver GASP [42]. About 460,000 and 400,000 simulated particles are used to represent gas molecules and clusters, respectively, at steady state.

Figure 7 compares the cluster number density contours in the condensation plume for the simulations using the kinetic (top) and CNT (bottom) nucleation models. It can be seen that the cluster number density contours for the simulation using CNT has much higher fluctuations than the contours obtained from the kinetic nucleation process. This is because in the kinetic model the initial clusters are created through a modified standard DSMC collision processes, whereas the distribution of initial clusters for the simulation using CNT is highly sensitive to the gas environment characteristics such as the degree of supersaturation S and gas temperature T. Note that even using larger numbers of simulated particles and samples, there is no significant improvement in the degree of fluctuations in the CNT simulations. Figure 7 shows that

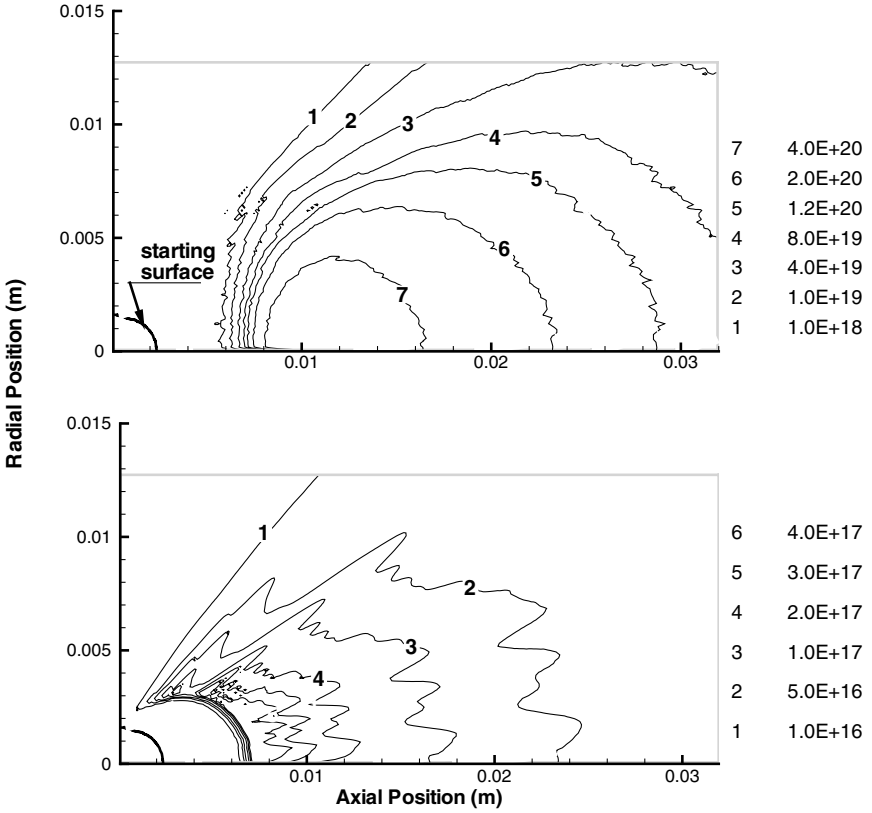

Fig. 7 Comparison of average cluster number density contours (m^{-3}) in a free-expanding condensation argon plume between the kinetic (top) and CNT (bottom) nucleation models.

the cluster number density obtained from the kinetic nucleation process is about three–four orders of magnitude larger than that from CNT.

Figure 8 compares contours of the average cluster size between the kinetic (top) and CNT (bottom) nucleation models. It can be seen that the average cluster size obtained from the kinetic nucleation process is smaller than the value obtained from the CNT nucleation process. The outcome of argon cluster–monomer collisions [28] can be described by average sticking probabilities as a function of cluster size, as shown in Fig. 9. According to these values, the average

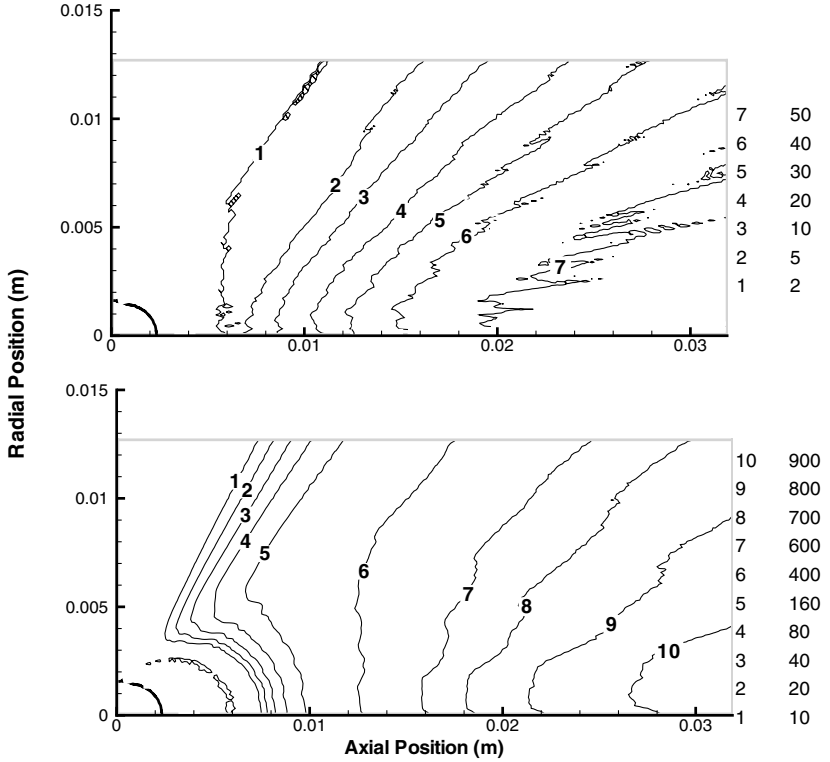

Fig. 8 Comparison of average cluster size (number of monomers) contours in a free-expanding condensation argon plume between the kinetic (top) and CNT (bottom) nucleation models.

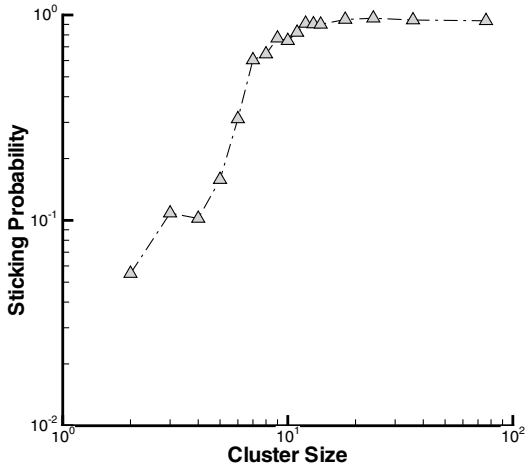

Fig. 9 Average argon cluster-monomer sticking probabilities from Zhong et al. [28].

sticking probability for a cluster size less than 11-mers increases quickly as the cluster size increases, whereas for cluster size larger than 10-mers, the sticking probability is very close to unity. The initial dimers generated in the kinetic nucleation process are difficult to grow through the dimer–monomer collision processes due to a small probability around 0.05. However, the CNT nucleation process define the critical clusters as the initial clusters, and the critical clusters can stick with the colliding monomers quickly due to large probabilities close to unity. Because large number of small clusters exist for the simulation using the kinetic nucleation process, its average cluster size can be more than 10 times less than the corresponding value obtained for the simulation using the CNT nucleation theory.

To quantitatively compare the kinetic and CNT nucleation process results, Fig. 10 shows the distributions of cluster number density and cluster size along the plume centerline. It can be seen from Fig. 10 that the initial clusters, dimers, in the kinetic nucleation process appear earlier than the initial critical clusters in the CNT simulation. The maximum cluster number density on the centerline shown in the kinetic nucleation simulation is at a position downstream of the location shown for the CNT simulation. For the simulation using the kinetic nucleation process, the maximum cluster number density on the centerline is about $8.0 \times 10^{+20}$ per cubic meter at the axial distance of 0.01 m downstream of the nozzle exit, whereas the CNT nucleation predicts the maximum cluster number density is about

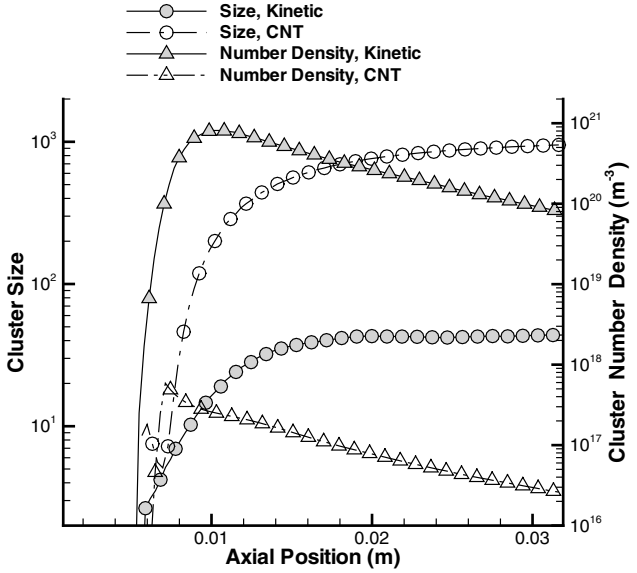

Fig. 10 Comparison of average cluster size and number density along the plume centerline between the kinetic and CNT nucleation models.

$3.0 \times 10^{+17}$ at the axial distance of 0.007 m. One possible reason is that the CNT neglects transient nuclei formation time [43], which would affect the generation location of nuclei in a supersaturated gas environment. Because of a large cluster number density and smaller initial cluster size, the cluster growth process is slower in the simulation using the kinetic nucleation process than the CNT nucleation process. At an axial position of 0.032 m, 10 nozzle throat diameters downstream from the nozzle exit, the average cluster size consists of approximately 950 molecules in the CNT simulation and 50 molecules in the kinetic simulation, whereas the cluster number density is about $2.72 \times 10^{+16}$ per cubic meter in the CNT simulation and $8.70 \times 10^{+19}$ in the kinetic simulation. Thus, it can be seen that the condensation results are quite different for the simulations using the kinetic and CNT nucleation processes.

Comparison with experiment substantiates that the proposed kinetic nucleation model for supersonic free expansions is a significant improvement over that given by CNT. To demonstrate this important result, we compare the predicted terminal cluster size and dimer mole fraction with the experimental data of [27,44], respectively. Karnbach et al. [44] used a photoluminescence spectroscopy technique consisting of a molecular beam and a cluster beam apparatus to measure the terminal average cluster size of a free-expanding condensation plume in a vacuum chamber. The experimental data suggest that the average cluster size is essentially a function of the condensation parameter Γ, which indicates the degree of condensation in a free-expanding plume as follows:

$$\Gamma = \frac{AP_0(d \times 1000)^{0.85}}{T_0^{2.2875}} \tag{11}$$

where P_0 is the stagnation pressure (mbar), T_0 is the stagnation temperature (K), and d is the throat diameter (mm). The constant A is calculated from the species sublimation enthalpy at 0 K and for argon has a value of 1646 [44]. Using the conditions of the simulations presented here in Eq. (11), we obtain a condensation parameter Γ of ∼658. The experimental data of [44] show that for a condensation parameter of this value, the average argon terminal cluster size will be approximately 30. As shown in Fig. 10, the kinetic nucleation model predicts an average cluster size close to the experimental results of about 50. The average cluster size predicted by the CNT nucleation model, however, is approximately 30 times larger than the experimental data. Thus, the kinetic nucleation model proposed in this work greatly improves the agreement with the simulation results.

Based on the available experimental data of free-expanding condensation jets, Knuth [27] proposed a simplified relationship for the terminal dimer mole fraction, χ_2, in a free-expanding argon jet as follows:

$$\chi_2 = 0.5\left\{\frac{P_0\sigma^3}{kT_0}\left(\frac{\epsilon}{kT_0}\right)^{1.4}\left(\frac{d}{\sigma}\right)^{0.4}\right\}^{\frac{5}{3}} \tag{12}$$

The dimer mole fraction is defined as the ratio of the number of dimers to the total number of gas and cluster particles. It was shown in [27] that the available experimental data are in good agreement with the semi-empirical relationship expressed in Eq. (12). First note that the CNT nucleation model predicts that the number of dimers anywhere in the flow is insignificant (see also Fig. 10). This occurs because in the CNT method the initial cluster is created at the critical cluster, which is usually much larger than a dimer. In contrast, there is a large number of dimers in the computational domain for the kinetic nucleation model because when a cluster is formed the dimer particles are created by the triple collision process. Figure 11 shows the average number of dimers as well as dimer mole fractions in a cell along the plume center line at steady state. It can be seen that the dimer mole fraction increases rapidly in the region from 0.006 to 0.01 m as large amounts of dimers are created from the local gas atoms. Beyond the high nucleation region, 0.012 m, the number of dimers decreases as other processes such as transport, expansion, and evaporation occur, although new dimer formation is continuing to occur. A typical cluster size distribution in the free-expanding condensation plume is shown in Fig. 12 in a cell located at

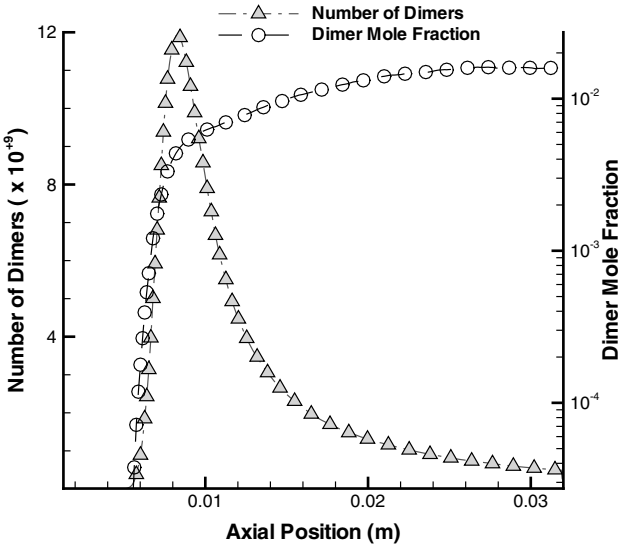

Fig. 11 The average number of dimers in a cell along the plume centerline, as well as dimer mole fractions at steady state.

$(1.72 \times 10^{-2},\ 3.0 \times 10^{-3})$. The location of this cell is at a point beyond the high nucleation onset region where the dimer mole fraction has reached its asymptotic or terminal value (as seen in Fig. 11). In the region beyond 0.012 m, the dimer mole fraction is approximately around 0.01, which is about 7 times greater than a value of 1.6×10^{-3} predicted by the semi-empirical relationship given in Eq. (12). Considering the level of complexity of the simulations the agreement between predictions and an experimentally derived fit is quite good. The residue difference may be due to our evaporation model, which is based on a macroscopic model that may be less accurate for small clusters such as dimers and trimers. The evaporation model may impact the lifetime for small clusters, which in turn would modify the predicted spatial distribution of dimers.

Based on the results, we may conclude that the CNT theory incorrectly estimates the nucleation rate to be three–four orders of magnitude less than the kinetic nucleation model for homogeneous condensation in a free-expanding argon plume. The fundamental difference between these two nucleation models is that CNT neglects the large number of small clusters which potentially can also grow to large clusters even though the small sticking collision probabilities for dimers are lower than those for large clusters. Because the existence of small clusters affects the cluster number density and average cluster size, the use of a kinetic nucleation model to accurately simulate a homogeneous condensation flow is crucial.

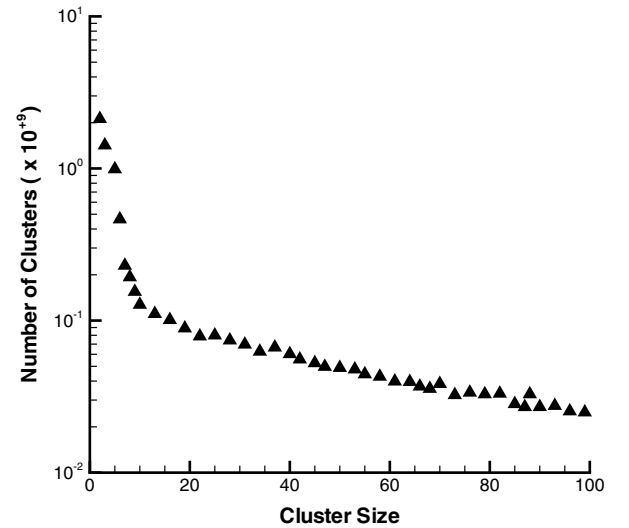

Fig. 12 A typical cluster distribution in the free-expanding condensation plume in a cell located at $(1.72 \times 10^{-2}, 3.0 \times 10^{-3})$.

V. Conclusions

A hybrid MD-DSMC method has been used to construct a kinetic nucleation model, generating initial clusters, dimers, from the triple collision processes. For argon gas environments with a large range in the degree of supersaturation, we calculate the lifetime of temporary binary complex formations, the stable dimer rate, triple-collision (complex-monomer) rate, and the probabilities of generation stable dimers out of triple collisions. The kinetic nucleation model has been successfully integrated into a DSMC code to simulate homogeneous condensation in free-expanding plumes.

In this work, we compare the numerical results between the kinetic and CNT nucleation processes in free-expanding sonic nozzle plumes with a stagnation temperature of 280 K and a stagnation pressure of 125 torr. The main difference of the kinetic and CNT nucleation processes is that the kinetic nucleation process produces a much larger number of small clusters, whereas the CNT nucleation process neglects cluster size less then the critical value. Thus for the condensation case studied in this work, the cluster number density for the simulation using the kinetic nucleation process is found to be three–four orders of magnitude larger and the average cluster size is about 20 times less than those values in the CNT nucleation process. The terminal cluster size and dimer mole fraction predicted in the kinetic nucleation model compares reasonably well to the semi-empirical value in argon free-expanding plumes. A possible source of discrepancy between modeling and simulation with experimental may be in the cluster evaporation model for small cluster sizes.

Acknowledgments

This work was supported by the Air Force Office of Scientific Research Grant No. F49620-02-1-0104, administered by Mitat Birkan, and the National Science Foundation CTS-0521968. The authors wish to express their gratitude to M. S. Ivanov for the use of SMILE and to L. V. Zhigilei for providing the computer code.

References

[1] Han, P., and Yoshida, T., "Growth and Transport of Clusters in Thermal Plasma Vapor Deposition of Silicon," *Journal of Applied Physics*, Vol. 92, No. 8, 2002, pp. 4772–4778.

[2] Saenger, K. L., "Pulsed Laser Deposition. 1. A Review of Process Characteristics and Capabilities," *Processing of Advanced Materials*, Vol. 3, No. 1, 1993, pp. 1–24.

[3] Selwyn, G., Singh, J., and Bennet, R., "In Situ Laser Diagnostic Studies of Plasma-Generated Particulate Contamination," *Journal of Vacuum Science and Technology A (Vacuum, Surfaces, and Films)*, Vol. 7, No. 4, 1989, pp. 2758–2765.

[4] Aizawa, M., Lee, S., and Anderson, S. L., "Sintering, Oxidation, and Chemical Properties of Size-Selected Nickel Clusters on TiO_2(110)," *Journal of Chemical Physics*, Vol. 177, No. 10, 2002, pp. 5001–5011.

[5] Aizawa, M., Luk'yanchuk, B. S., Marine, W., Anisimov, S. I., and Simakina, G. A., "Condensation of Vapor and Nanoclusters Formation Within the Vapor Plume, Produced by ns-Laser Ablation of Si, Ge and C," *Proceedings of SPIE: The International Society for Optical Engineering*, Vol. 3618, July 1999, pp. 434–452.

[6] Xirouchaki, C., and Palmer, R. E., "Deposition of Size-Selected Metal Clusters Generated by Magnetron Sputtering and Gas Condensation: A Progress Review," *Philosophical Transactions of the Royal Society of London, Series A: Mathematical and Physical Sciences*, Vol. 362, No. 1814, 2004, pp. 117–124.

[7] Ashfold, M., Claeyssens, F., Fuge, G., and Henley, S., "Pulsed Laser Ablation and Deposition of Thin Films," *Chemical Society Reviews*, Vol. 33, No. 1, 2004, pp. 23–32.

[8] Williams, W. D., and Lewis, J. W. L., "Summary Report for the CONTEST Program at AEDC," Arnold Engineering Development Center TR-80-16, Arnold AFB, TN, Sept. 1980.

[9] Alexeenko, A. A., Wadsworth, D. C., Gimelshein, S. F., and Ketsdever, A. D., "Numerical Modeling of ISS Thruster Plume Induced Contamination Environment," *Proceedings of SPIE: The International Society for Optical Engineering*, Vol. 5526, Aug. 2004, pp. 125–136.

[10] Harvey, G., "Thruster Residues on Returned Mir Solar Pannel,"

Proceedings of SPIE: The International Society for Optical Engineering, Vol. 4096, Aug. 2000, pp. 41–47.

[11] Ishiyama, T., Yano, T., and Fujikawa, S., "Molecular Dynamics Study of Kinetic Boundary Condition at an Interface Between Argon Vapor and its Condensed Phase," *Physics of Fluids*, Vol. 16, No. 8, 2004, pp. 2899–2906.

[12] Meland, R., Frezzotti, A., Ytrehus, T., and Hafskjold, B., "Nonequilibrium Molecular-Dynamics Simulation of Net Evaporation and Net Condensation, and Evaluation of the Gas-Kinetic Boundary Condition at the Interphase," *Physics of Fluids*, Vol. 16, No. 2, 2004, pp. 223–243.

[13] Frezzotti, A., and Ytrehus, T., "Kinetic Theory Study of Steady Condensation of a Polyatomic Gas," *Physics of Fluids*, Vol. 18, No. 2, 2006, pp. 027101-1–12.

[14] Bird, G. A., *Molecular Gas Dynamics and the Direct Simulation of Gas Flows*, Oxford Science Publications, Oxford, 1994.

[15] Zhong, J., Gimelshein, S. F., Zeifman, M. I., and Levin, D. A., "Direct Simulation Monte Carlo Modeling of Homogeneous Condensation in Supersonic Plumes," *AIAA Journal*, Vol. 43, No. 8, 2005, pp. 1784–1796.

[16] Zhong, J., Zeifman, M. I., and Levin, D. A., "Sensitivity of Water Condensation in a Supersonic Plume to the Nucleation Rate," *Journal of Thermophysics and Heat Transfer*, Vol. 20, No. 3, 2006, pp. 517–523.

[17] Abraham, F. F., *Homogeneous Nucleation Theory*, Academic Press, New York, 1974, p. 263.

[18] Itkin, A. L., and Kolesnichenko, E. G., *Microscopic Theory of Condensation in Gases and Plasma*, World Scientific Publishing, Singapore, 1997, p. 273.

[19] Kathmann, S. M., Schenter, G. K., and Garrett, B. C., "Understanding the Sensitivity of Nucleation Kinetics: A Case Study on Water," *Journal of Chemical Physics*, Vol. 116, No. 12, 2002, pp. 5046–5057.

[20] Yasuoka, K., and Matsumoto, M., "Molecular Dynamics of Homogeneous Nucleation in the Vapor Phase. 1. Lennard-Jones Fluid," *Journal of Chemical Physics*, Vol. 109, No. 19, 1998, pp. 8451–8462.

[21] Senger, B., Schaaf, P., Corti, D. S., Bowles, R., Pointu, D., Voegel, J. C., and Reiss, H., "A Molecular Theory of the Homogeneous Nucleation Rate. 2. Application to Argon Vapor," *Journal of Chemical Physics*, Vol. 110, No. 13, 1999, pp. 6438–6450.

[22] Sharaf, M. A., and Dobbins, R. A., "A Comparison of Measured Nucleation Rate with the Predictions of Several Theories of Homogeneous Nucleation," *Journal of Chemical Physics*, Vol. 77, No. 3, 1982, pp. 1517–1526.

[23] Schenter, G. K., Kathmann, S. M., and Garrett, B. C., "Variational Transition State Theory of Vapor Phase Nucleation," *Journal of Chemical Physics*, Vol. 110, No. 16, 1999, pp. 7591–7559.

[24] Haberland, H., *Clusters of Atoms and Molecules*, edited by H. Haberland, Springer, Berlin, 1994, p. 207.

[25] Zeifman, M. I., Zhong, J., and Levin, D. A., "A Hybrid MD-DSMC Approach to Direct Simulation of Condensation in a Supersonic Jets," AIAA Paper 2004-2586, June 2004.

[26] Zhong, J., Zeifman, M. I., and Levin, D. A., "Direct Simulation of Condensation in a One-Dimensional Unsteady Expansion: Microscopic Mechanisms," *Physics of Fluids*, Vol. 17, No. 12, 2005, pp. 128102-1–4.

[27] Knuth, E. L., "Dimer-Formation Rate Coefficients from Measurements of Terminal Dimer Concentrations in Free-Jet Expansions," *Journal of Chemical Physics*, Vol. 66, No. 8, 1977, pp. 3515–3525.

[28] Zhong, J., Zeifman, M. I., and Levin, D. A., "A Kinetic Model of Condensation in a Free Argon Expanding Jet," *Journal of Thermophysics and Heat Transfer*, Vol. 20, No. 1, 2006, pp. 41–51.

[29] Benson, C. M., Zhong, J., Gimelshein, S. F., Levin, D. A., and Montaser, A., "Simulation of Droplet Heating and Desolvation in an Inductively Coupled Plasma—Part 2: Coalescence in the Plasma," *Spectrochimica Acta, Part B: Atomic Spectroscopy*, Vol. 58, No. 8, 2003, pp. 1453–1471.

[30] Boyd, I. D., "Analysis of Vibration-Dissociation-Recombination Processes Behind Strong Shock Waves of Nitrogen," *Physics of Fluids A*, Vol. 4, No. 1, 1992, pp. 178–185.

[31] Gimelshein, S. F., Levin, D. A., Drakes J. A, Karabadzhak, G. F., and Ivanov, M. S., "Ultraviolet Radiation Modeling from High-Altitude Plumes and Comparison with Mir Data," *AIAA Journal*, Vol. 41, No. 4, 2004, pp. 582–591.

[32] Koura, K., "A Set of Model Cross Sections for the Monte Carlo Simulation of Rarefied Real Gases: Atom-Diatom Collisions," *Physics of Fluids*, Vol. 105, No. 14, 2001, pp. 3454–3457.

[33] Frenkel, D., and Smit, B., *Understanding Molecular Simulation: From Algorithms to Applications*, Academic Press, San Diego, CA, 1996.

[34] Stillinger, F. H., "Rigorous Basis of the Frenkel-Band Theory of Association Equilibrium," *Journal of Chemical Physics*, Vol. 38, No. 4, 1963, pp. 1486–1494.

[35] Bunker, D. L., "Mechanics of Atomic Recombination Reactions," *Journal of Chemical Physics*, Vol. 32, No. 4, 1960, pp. 1001–1005.

[36] Kalus, R., "Formation of Argon Dimers in Ternary Monomer Collisions-A Classical Trajectory Study," *Journal of Chemical Physics*, Vol. 109, No. 19, 1998, pp. 8289–8294.

[37] Soto, R., and Cordero, P., "Cluster Birth-Death Processes in a Vapor at Equilibrium," *Journal of Chemical Physics*, Vol. 110, No. 15, 1999, pp. 7316–7325.

[38] Bernshtein, V., and Oref, I., "Dependence of Collision Lifetimes on Translational Energy," *Journal of Physical Chemistry A*, Vol. 105, No. 14, 2001, pp. 3454–3457.

[39] Ivanov, M. S., Markelov, G. N., and Gimelshein, S. F., "Statistical Simulation of Reactive Rarefied Flows: Numerical Approach and Application," AIAA Paper 98-2669, June 1998.

[40] Gimelshein, S. F., Levin, D. A., Drakes, J. A., Karabadzhak, G. E., and Ivanov, M. S., "Ultraviolet Radiation Modeling from High-Altitude Plumes and Comparison with Mir Data," *AIAA Journal*, Vol. 38, No. 12, 2000, pp. 2344–2352.

[41] Zhong, J., "Modeling of Homogeneous Condensation in Free-Expanding Plumes with the Direct Simulation Monte Carlo Method," Ph.D. Thesis, Pennsylvania State University, University Park, PA, 2005.

[42] The General Aerodynamic Simulation Program, GASP Ver. 4.1, Computational Flow Analysis Software for the Scientist and Engineer, User's Manual, Aersoft, Inc., Blacksburg, VA.

[43] Wu, D. T., "The Time Lag in Nucleation Theory," *Journal of Chemical Physics*, Vol. 97, No. 4, 1992, pp. 2644–2650.

[44] Karnbach, R., Joppien, M., Stapelfeldt, J., Wormer, J., and Moller, T., "CLULU: An Experimental Setup for Luminescence Measurements on van der Waals Clusters with Synchrotron Radiation," *Review of Scientific Instruments*, Vol. 64, No. 10, 1993, pp. 2838–2849.

C. Kaplan
Associate Editor